ELSEVIER

Journal of Nuclear Materials 304 (2002) 134–138

journal of nuclear materials

www.elsevier.com/locate/jnucmat

Determination of Fe and Cr content in α-Zr solid solution of Zircaloy-4 with different heat-treated states

Cong Li [a,b,*], Bangxin Zhou [a], Wenjin Zhao [a], Pei Li [a], Qian Peng [a], Shihao Ying [a], Baoluo Shen [b]

[a] National Key Laboratory for Nuclear Fuel and Materials, Nuclear Power Institute of China, P.O. Box 436, Chengdu, Sichuan 610041, People's Republic of China

[b] School of Materials Science and Engineering, Sichuan University, Chengdu, Sichuan 610065, People's Republic of China

Received 18 December 2001; accepted 17 May 2002

Abstract

A new method, which is a combination of extracting electrochemically $Zr(Fe,Cr)_2$ particles from Zircaloy-4 and analyzing mass concentration in electrolyte by means of flame atomic absorption spectrometry, has been successfully established and used to determine the content of alloying elements Fe and Cr in α-Zr solid solution of Zircaloy-4 with different heat treatments. Along with the Fe/Cr ratio in α-Zr solid solution, the Fe and Cr content in α-Zr solid solution of β quenched sample is higher than that of α + β quenched sample, and the α-annealed sample has the lowest content, comparable to the solubility limits of Fe and Cr in α-Zr solid solution. Both Fe and Cr contents in the quenched states are much higher than its maximal solubility limit in α-Zr solid solution respectively.

1. Introduction

Zircaloy is used as the cladding material of fuel elements in light water reactors, and Zircaloy resistance to waterside corrosion limits the lifetime of fuel elements. The current trend to extend fuel burn-up and to uprate the reactor power will result in even heavier Zircaloy corrosion. Thus, there exists an incentive to improve the corrosion resistance.

It is well known that the corrosion resistance of Zircaloy can be improved by optimizing the thermo-mechanical processing. In the fabrication process, some alloying elements precipitate as the second phase particles, and their remainder still is in the α-Zr solid solution as solute atoms. The contribution of thermo-mechanical processing to the corrosion resistance has been found to correlate well with the distributions of alloying elements, i.e. the morphology of second phase particles and the content of alloying elements supersaturated in α-Zr solid solution. However, there is no general agreement on the cause of the impact of the distributions on the corrosion resistance. Some authors attributed it to the morphology [1–5], while others believed that the content of alloying elements supersaturated in α-Zr solid solution was a main factor affecting the resistance [6–9].

Hence, in order to gain a further insight into the causes involved, it is necessary to investigate the variations of Fe and Cr content in α-Zr solid solution of Zircaloy-4. There are two methods described by other researchers to get the Fe and Cr content in α-Zr solid solution. One is using atom probe microanalysis [10], this method is rather time consuming in the authors' and others experiences, especially the tip of testing sample for zirconium alloys is inclined to fracture, which make the

---

[*] Corresponding author. Address: National Key Laboratory for Nuclear Fuel and Materials, Nuclear Power Institute of China, P.O. Box 436, Chengdu, Sichuan 610041, People's Republic of China. Tel.: +86-28 8558 2199x33379; fax: +86-28 8558 2223.

E-mail address: licong@npic.ac.cn (C. Li).

0022-3115/02/$ - see front matter © 2002 Elsevier Science B.V. All rights reserved.
PII: S0022-3115(02)00882-6

experiment difficult to perform. Another technique is measuring the variation of thermoelectric power [11], and this method is not capable of determining high content of Fe and Cr supersaturated in α-Zr solid solution.

The paper herein describes a new method to determine the Fe and Cr content in α-Zr solid solution of Zircaloy-4.

2. Experimental principle and procedure

2.1. Principle

$Zr(Fe,Cr)_2$ particles were successfully extracted electrochemically from Zircaloy-4 plates [12]. This is based upon the following principle: In Zircaloy-4, the $Zr(Fe,Cr)_2$ particles are more noble than the α-Zr solid solution, therefore, the oxidation–reduction system between α-Zr solid solution and $Zr(Fe,Cr)_2$ particles forms in a electrolyte under certain condition, which leads to the dissolution of α-Zr solid solution while $Zr(Fe,Cr)_2$ particles remain unchanged as cathode. It means that the ions Zr, Sn, Fe and Cr in the electrolyte only come from the α-Zr solid solution. Thus there exists following equations:

$$C_{\mathrm{Fe}} = C_{\mathrm{Sn}}\frac{[\mathrm{Fe}]}{[\mathrm{Sn}]}, \tag{1}$$

$$C_{\mathrm{Cr}} = C_{\mathrm{Sn}}\frac{[\mathrm{Cr}]}{[\mathrm{Sn}]}, \tag{2}$$

where C_X collectively designates the content of alloying elements Zr, Sn, Fe and Cr in α-Zr solid solution of Zircaloy-4 and $[X]$ designates the concentration of ion X in the electrolyte. Considering that Zircaloy-4 consists of the alloying elements Zr, Sn, Fe and Cr, the content of Fe and Cr in the α-Zr solid solution can be evaluated by the following equation:

$$C_{\mathrm{Fe+Cr}} = \frac{[\mathrm{Fe}]+[\mathrm{Cr}]}{[\mathrm{Zr}]+[\mathrm{Sn}]+[\mathrm{Fe}]+[\mathrm{Cr}]}. \tag{3}$$

However, [Zr], [Sn], [Fe] and [Cr] are hard to be accurately measured because [Zr] is much larger than [Fe] + [Cr].

To solve this problem, an attention is given to both the alloying element Sn and the second phase particles. In Zircaloy-4, Sn is fully in α-Zr solid solution at the usual composition [10], leading to the following equation:

$$C^0_{\mathrm{Sn}} = (1-\chi)C_{\mathrm{Sn}}, \tag{4}$$

where χ is the mass fraction of second phase particles, C^0_X collectively designates the chemical composition of alloying elements Zr, Sn, Fe and Cr in Zircaloy-4. Furthermore, the second phase particles has a stoichiometry of $Zr(Fe,Cr)_2$, and the concentration of the alloying elements Fe and Cr are in the range of 0.18–0.24 and 0.07–0.13 mass%, respectively. Therefore χ is not more than 0.68% and C_{Sn} could be taken as C^0_{Sn}, with a maximum relative uncertainty of less than 0.68%. Thus, Eqs. (1) and (2) can be written as follows:

$$C_{\mathrm{Fe}} = C^0_{\mathrm{Sn}}\frac{[\mathrm{Fe}]}{[\mathrm{Sn}]}, \tag{5}$$

$$C_{\mathrm{Cr}} = C^0_{\mathrm{Sn}}\frac{[\mathrm{Cr}]}{[\mathrm{Sn}]}. \tag{6}$$

Of course,

$$C_{\mathrm{Fe+Cr}} = C_{\mathrm{Fe}} + C_{\mathrm{Cr}}. \tag{7}$$

In addition, the value χ is derived from the following equation in light of the structural formula $Zr(Fe,Cr)_2$,

$$2\frac{C^0_{\mathrm{Zr}} - C_{\mathrm{Zr}}(1-\chi)}{M_{\mathrm{Zr}}} = \frac{C^0_{\mathrm{Fe}} - C_{\mathrm{Fe}}(1-\chi)}{M_{\mathrm{Fe}}} + \frac{C^0_{\mathrm{Cr}} - C_{\mathrm{Cr}}(1-\chi)}{M_{\mathrm{Cr}}}, \tag{8}$$

where $C^0_{\mathrm{Zr}} = 1-(C^0_{\mathrm{Sn}}+C^0_{\mathrm{Fe}}+C^0_{\mathrm{Cr}})$, similarly $C_{\mathrm{Zr}} = 1-(C_{\mathrm{Sn}}+C_{\mathrm{Fe}}+C_{\mathrm{Cr}})$, and M_X collectively designates the atomic weight of Zr, Fe and Cr, which are 91.22, 55.85 and 52.00, respectively. Consequently, the Fe/Cr ratio in $Zr(Fe,Cr)_2$ particles, R_{P}, is expressed as

$$R_{\mathrm{P}} = \frac{C^0_{\mathrm{Fe}} - C_{\mathrm{Fe}}(1-\chi)}{C^0_{\mathrm{Cr}} - C_{\mathrm{Cr}}(1-\chi)}. \tag{9}$$

2.2. Material

In order to avoid the impact of the variation of alloy compositions on the values C_{Fe} and C_{Cr}, the samples used in this test come from a single ingot, whose composition is given in Table 1. The heat treatments are shown in Table 2. The fabrication routes and microstructural characterizations for these samples had been described in detail previously [13].

2.3. Electrolytic dissolution

At room temperature, the sample as working electrode is immerged in an electrolyte made of a mixture of

Table 1
Chemical composition of the material, where the relative standard deviation (RSD) for Sn, Fe and Cr are 1.0%, 8.0%, 8.0%, respectively

	Alloying element		
	Sn	Fe	Cr
Content (mass%)	1.36	0.19	0.12

Table 2
Heat-treatment schedule of samples

Sample	Penultimate annealing	Final annealing temperature	Tube size (mm)
A	1030 °C – 1.5 h quenching in water	470 °C – 4 h	∅ 9.5 × 0.64
B	830 °C – 1.5 h quenching in water	470 °C – 4 h	∅ 9.5 × 0.64
C	650 °C – 2 h annealing and furnace cooling	470 °C – 4 h	∅ 9.5 × 0.64

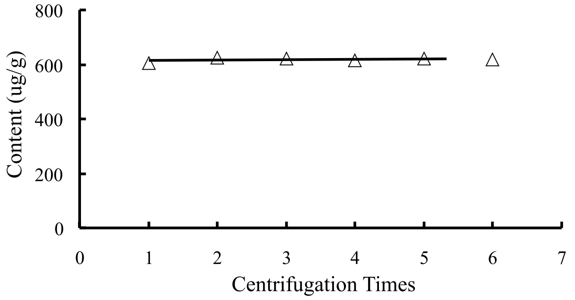

Fig. 1. The value C_{Fe+Cr} versus centrifugation times, corresponding to the sample heated at 1030 °C for 0.5 h followed by air-cooling.

ethanol, perchloric acid and butanol (ethanol:perchloric acid:butanol = 25:3:2, vol), at an operating voltage in the range −0.80 to −0.45 V (SCE). The α-Zr solid solution dissolves as anode, meanwhile $Zr(Fe,Cr)_2$ particles remain unchanged as cathodes.

If there exist some $Zr(Fe,Cr)_2$ particles in the electrolyte, the values C_{Fe}, C_{Cr} and C_{Fe+Cr}, calculated by Eqs. (5)–(7), would be higher. So, in order to have the $Zr(Fe,Cr)_2$ particles completely removed from the electrolyte a centrifugation process was used. It can be seen from Fig. 1 that the centrifugation times has little effect on the value C_{Fe+Cr} for the centrifugation conditions chosen. The optimal conditions are 3000 rpm and 20 min to acquire the electrolyte without solid products.

X-ray diffraction analysis is applied to investigate the centrifugal solid products to confirm that $Zr(Fe,Cr)_2$ particles have been extracted successfully from the samples.

2.4. Analysis of electrolyte

Because [Sn], [Fe] and [Cr] are in the level of μg/dm³, they are measured by flame atomic absorption spectrometry (FAAS).

3. Experimental results

3.1. X-ray diffraction analysis

Fig. 2 depicts the X-ray diffraction spectrum of centrifugation solid products from electrolyte of sample A.

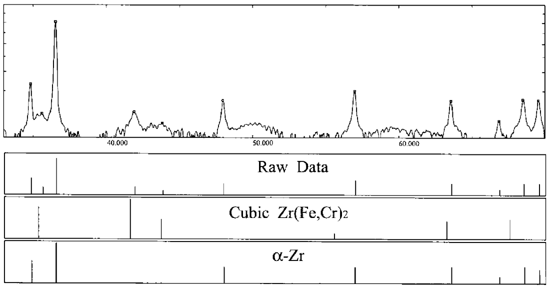

Fig. 2. X-ray diffraction spectrum for centrifugate of sample A.

As can be seen from the spectrum, there appears α-Zr in addition to $Zr(Fe,Cr)_2$. Centrifugal solid products of samples B and C are also made up of α-Zr and $Zr(Fe,Cr)_2$. $Zr(Fe,Cr)_2$ particles in sample A are cubic fcc (structure type C15). However, those in samples B and C are hexagonal hcp (C14). These findings agree well with the results obtained by using selected area electron diffraction [13].

It indicates that $Zr(Fe,Cr)_2$ particles have been successfully extracted from the samples, and that some α-Zr matrix dissolve incompletely in the electrolyzing process.

3.2. Fe and Cr content in α-Zr solid solution

The measured [Sn], [Fe] and [Cr] in the centrifugated electrolyte are shown in Table 3.

On the basis of Tables 1 and 3 and Eqs. (5)–(7), the values C_{Fe}, C_{Cr} and C_{Fe+Cr} along with the Fe/Cr ratio in α-Zr solid solution, R_M, are calculated, which are given in Table 4. Therefore, the values χ and R_P are calculated and also shown in Table 4.

Table 3
Measured concentration of ions in the centrifugated electrolyte

Concentration (μg/dm³)	Sample		
	A	B	C
[Sn] %RSD	163	203.1	249.7
	1.35	0.28	0.30
[Fe] %RSD	12.0	7.86	2.83
	0.79	0.23	0.31
[Cr] %RSD	3.6	3.77	3.0
	3.74	0.93	4.09

Table 4
Analysis results for samples

Results	Sample		
	A	B	C
C_{Fe} (μg/g)	1001 ± 19	526 ± 6	154 ± 2
C_{Cr} (μg/g)	300 ± 12	252 ± 4	163 ± 7
$C_{\mathrm{Fe+Cr}}$ (μg/g)	1301 ± 22	778 ± 7	317 ± 7
R_{M}	3.33 ± 0.15	2.08 ± 0.04	0.94 ± 0.04
χ (mass%)	0.34 ± 0.03	0.43 ± 0.03	0.52 ± 0.03
R_{P}	1.00 ± 0.22	1.45 ± 0.21	1.68 ± 0.20

From Table 4, the difference in $C_{\mathrm{Fe+Cr}}$ between samples can be seen. In sample A, $C_{\mathrm{Fe+Cr}}$ is the highest, more than one third of the alloying elements Fe and Cr are supersaturated in α-Zr solid solution, meanwhile R_{M} is the highest, both χ and R_{P} are the lowest correspondingly. In sample C, $C_{\mathrm{Fe+Cr}}$ is the lowest, both C_{Fe} and C_{Cr} are comparable to the solubility limit in α-Zr solid solution respectively [14,15], only one tenth of Fe and Cr is in the α-Zr solid solution, and R_{M} is also the lowest, however both χ and R_{P} are the highest. Sample B lies between samples A and C regarding these values.

4. Discussion

Some comparisons can be made usefully with the findings of Wadman et al. [16], obtained by using atom probe microanalysis. In their sample 3–1, $C_{\mathrm{Fe+Cr}}$ was 360 μg/g, slightly different from that in present sample C, and both samples are similar regarding the fabrication route. The processing of both samples is not identical, and it is possible that this accounts for the difference in $C_{\mathrm{Fe+Cr}}$. In addition, in their β-quenched Zircaloy-4 sample, which was heated up to 1080 °C in vacuum followed by rapid cooling to room temperature in helium gas, $C_{\mathrm{Fe+Cr}}$ was 500 μg/g, lower than that in sample A. It could be attributed to the fact that the cooling rate in helium gas is slower than that in water, so that more $Zr(Fe,Cr)_2$ particles precipitate, leading to less $C_{\mathrm{Fe+Cr}}$.

Another comparison shows that the results presented in Table 4 are consistent with the results obtained by Godlewski [17], who used electron micro-probe to investigate R_{P} in Zircaloy-4 samples from the same batch. His findings indicated that the values R_{P} for both stress relief and recrystallized samples were 1.6 (at), and decreased to 0.8 (at) for β quenching. Moreover, an investigation of energy dispersive X-ray analyzer (EDX) also showed that the calculated values R_{P}, given in Table 4, agreed well with the Fe/Cr ratios in the extracted $Zr(Fe,Cr)_2$ particles.

Furthermore, a comparison between the present samples is made for the values R_{M}, presented in Table 4. For both the samples A and B, R_{M} becomes higher than the ratio of alloying elements Fe and Cr in the alloy. These are due partially to the difference in the diffusion rates between Fe and Cr in the β phase, where Fe diffuses faster than Cr [18]. This leads Fe to concentrate preferentially in the residual β phase during the later stages of the β–α transformation. In other words, fewer Fe atoms remain in the α phase and more Fe atoms remain in the residual β phase. Therefore much Fe atoms remained in the residual β phase are supersaturated in the α solid solution when the residual β phase transforms into α phase at a high rate. So, $Zr(Fe,Cr)_2$ particles precipitated from α phase possess less Fe/Cr ratio. Sample A thus shows the highest R_{M}, the lowest R_{P}, correspondingly.

The corrosion resistance described in [13] with the values C_{Fe}, C_{Cr} and $C_{\mathrm{Fe+Cr}}$, given in Table 4, shows that more Fe and Cr supersaturated in α-Zr solid solution corresponds to a better corrosion resistance. Hence, more Fe and Cr supersaturated in α-Zr solid solution might play an important role in the corrosion resistance of Zircaloy-4.

5. Conclusions

A new method, based on extracting electrochemically $Zr(Fe,Cr)_2$ particles from Zircaloy-4 and analyzing mass concentration of centrifugated electrolyte by means of FAAS, can be used for determining Fe and Cr content in α-Zr solid solution of Zircaloy-4.

Along with the Fe/Cr ratio in α-Zr solid solution, the Fe and Cr content in α-Zr solid solution of β quenched sample is higher than that of α + β quenched sample, and the α-annealed sample has the lowest solute content, comparable to the solubility limits of Fe and Cr in α-Zr solid solution. Both Fe and Cr contents in the quenched states are much higher than its maximal solubility limits in α-Zr solid solution respectively.

Acknowledgements

We would like to thank Professor Zhongqi Sheng for useful discussion.

References

[1] F. Garzarolli et al., IAEA STI/PUB/721, International Atomic Energy Agency, Vienna, 1987, p. 387.

[2] G. Garzarolli et al., in: Zirconium in the Nuclear Industry, Eighth International Symposium, ASTM STP 1023, American Society for Testing and Materials, Philadelphia, PA, 1989, p. 202.

[3] P. Rudling et al., in: Zirconium in the Nuclear Industry, Tenth International Symposium, ASTM STP 1245,

American Society for Testing and Materials, Philadelphia, PA, 1994, p. 599.
[4] P. Rudling et al., J. Nucl. Mater. 265 (1999) 44.
[5] D. Charquet, in: Zirconium in the Nuclear Industry, Twelfth International Symposium, ASTM STP 1354, American Society for Testing and Materials, West Conshohocken, PA, 2000, p. 3.
[6] B. Cheng et al., in: Zirconium in the Nuclear Industry, Seventh International Symposium, ASTM STP 939, American Society for Testing and Materials, Philadelphia, PA, 1987, p. 387.
[7] C.T. Wang et al., in: Zirconium in the Nuclear Industry, Ninth International Symposium, ASTM STP 1132, American Society for Testing and Materials, Philadelphia, PA, 1991, p. 319.
[8] D.F. Taylor, J. Nucl. Mater. 184 (1991) 65.
[9] D.F. Taylor, J. Nucl. Mater. 277 (2000) 295.
[10] B. Wadman et al., in: Zirconium in the Nuclear Industry, Eighth International Symposium, ASTM STP 1023, American Society for Testing and Materials, Philadelphia, PA, 1989, p. 423.
[11] K. Loucif et al., J. Nucl. Mater. 202 (1993) 193.
[12] X. Yang et al., Nucl. Power Eng. 15 (1) (1994) 79 (in Chinese).
[13] B. Zhou et al., China Nuclear Science and Technology Report, CNIC-01074, SINRE-0066, 1996.
[14] R. Borrelly et al., J. Nucl. Mater. 170 (1990) 147.
[15] H. Okamoto, J. Phase Equil. 14 (1993) 768.
[16] B. Wadman et al., J. Nucl. Mater. 200 (1993) 207.
[17] J. Godlewski, in: Zirconium in the Nuclear Industry, Tenth International Symposium, ASTM STP 1245, American Society for Testing and Materials, Philadelphia, PA, 1994, p. 663.
[18] H. Blank, J. Nucl. Mater. 240 (1997) 169.